



8th International Congress of Information and Communication Technology, ICICT 2019

Adaptive Wide-Lens Distortion Correction Based on Piecewise Polynomial Optimization

Rui Qing Wu*¹, Jian Liu, Wei Chen, Qing Shui Gu

School of Information Communication Engineering, University of Electronic Science and Technology of China, Chengdu China 611731

Abstract

An adaptive piecewise low-order mapping method that automatically extracts control point pairs from single orthogonal grid pattern is proposed to correct serious wide-lens distortion. Firstly, distorted control points (DCPs) are located by oriented searching along crossing lines in thinned grid image, and the relative distribution relationship between DCPs is obtained to estimate ideal control points in normalized grid pattern. Subsequently, a piecewise polynomial optimization problem, which minimizes two cost functions, is built to model whole radial distortion, thus adaptive pieces and corresponding segmented coefficients are optimized. Finally, an inverse mapping table is established to improve correction efficiency. Experimental results illustrate that the proposed method is effective and practical for high resolution wide-angle lens with perfect precision, and completely preserves the undistorted image edge.

© 2019 The Authors. Published by Elsevier Ltd.

This is an open access article under the CC BY-NC-ND license (<https://creativecommons.org/licenses/by-nc-nd/4.0/>)

Selection and peer-review under responsibility of the 8th International Congress of Information and Communication Technology, ICICT 2019.

Keywords Automatic extraction; control point pairs; distortion correction; piecewise polynomial; wide-angle lens

I. Introduction

Compared with images taken by ordinary cameras, images from wide-angle lens contain more information in a wider range of view owing to shorter focal length, larger view and deeper field. Therefore, wide-angle cameras have been widely used in video surveillance, semi-automatic parking, auxiliary driving, endoscopic imaging and other computer vision fields [1-2]. However, due to nonlinear geometric imaging structure, images captured by wide-angle

¹ * Corresponding author. Tel.:+(86) 18190708600

Email: rquwu@uestc.edu.cn

cameras suffer from serious barrel distortion [3] including decentering distortion, thin prism distortion and radial distortion [4]. Radial distortion is the typical distortion that displaces pixels points towards the principal intersection point that lens optical axis passes through the image[5], which twists the original image geometry. Only such distortion is corrected, can wide-angle lens really apply to practical requirements [6]. To overcome this issue, an increasing number of research works have been carried out. In Tsai's two-step method [7], a radial distortion model was presented and corresponding points known in 3D space were utilized to recover distortion parameters. Based on Tsai's method, Junhee Park et al [8] proposed a distortion model defined on ideal undistorted coordinates to achieve fast and simple lens mapping. Zhang [9] used planar chessboard pattern taken from different orientations to calibrate intrinsic parameters of camera and calculate distortion coefficients. Fitzgibbon [10] presented the prestigious division distortion model with just a single parameter, which is suitable to model most lenses with high distortion. Under the single parameter division model, Aiqi Wang et al [11] presented a simple method to determine the distortion function based on single image. Nonparametric distortion model [12] also has been raised recently. [13] adopted quartic polynomial to fit radial distortion, which compensates distortion in all types of lenses with low or high distortion. These parameter-free correction methods require correspondences between the input image and calibration pattern, which usually requires user interaction [14]. What's more, the novel line-based calibration method [14-16] is another powerful choice, which is partially suitable in structured environments or straight-lines patterns [17]. This approach utilizes the geometric invariant principle that ideal geometry of distorted lines in image plane projected from the 3D world is supposed to be straight.

These existing methods are effective to correct distorted lens images. However, they had disadvantages in restoring the image edge for high-resolution lens. Some methods using structured pattern require the availability of the corresponding ideal reference pattern, and others algorithms need user interaction to obtain control point pairs. Therefore, we propose an adaptive piecewise low-order mapping correction method based on single grid pattern, which extracts control point pairs automatically and is practical for seriously distorted wide-lens correction with high precision.

2. Distortion Calibration

2.1 Extract control point pairs

Due to high dynamic range, wide-lens images become fuzzy and dark in out-of-focus edges especially when they are captured in uneven environmental illumination, the general global binarization algorithm cannot achieve ideal segmentation effect. Furthermore, it causes serious problems, such as line breakage, burring boundary and serious edge noise. Therefore, block binarization method via OTSU using small blocks with different sizes, median filtering and connected-field casting are presented to obtain better segmentation result. Intersection points of grid lines are extracted to obtain the correspondence between distortion and ideal coordinates. It's noted that common corners extraction algorithm, such as Harris method, results in imprecise or missing detection in out-of-focus regions of grid pattern, because it only utilize a unified threshold parameter which is also not easy to select artificially. Therefore, we propose a novel approach processed in thinned binary grid image to extract accurate and precise grid intersections. Combined with oriented searching along grid lines in four areas, the ideal coordinates of grid intersections can be calculated.

1. Establish the relative distribution relationship coordinate system (DRCS) shown in Fig. 1, which indicates relative distribution between grid intersections in ideal grid pattern. It's meant that $P(0,0)$ is the grid intersection nearest to the center of the thinned grid image.

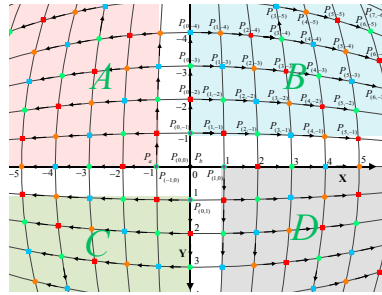


Fig. 1 DRCS for extracting grid intersections

2. Extract distorted intersections and their relative distribution in DRCS by oriented searching in four areas respectively, marked with square A, B, C and D in Fig. 1. Grid intersections can be located precisely through the extension direction and structure of lines in neighbor block of the candidate intersection along the search direction. Because grid lines are jagged in out-of-focus regions, some grid intersections are split into two adjacent intersections, in which case their midpoint is regarded as the detected intersection. Distortion direction is different from each other in the four areas, so that we divide the whole grid image into several area blocks with different search direction, seen in Fig. 1. For example, the searching algorithm in top-right area B is processed as follows:

- (1) Let S_{search} denote a set consisting of sequential points, and initialize the search set S_{search} with $P_{(0,-1)}$, ie. $S_{search} = \{P_{(0,-1)}\}$;
 - (2) If S_{search} is empty, then quit and get result;
 - (3) For each search point in S_{search} , if it is the first seed, then search the next adjacent intersections along the grid line upward and rightward, otherwise only search rightward;
 - (4) Obtain the relative distribution coordinate (rd_{Cor}) of each intersection detected in (3) according to each reference point and search direction in DRCS;
 - (5) Update S_{search} with all intersections searched in (3), and turn to (2).
3. Ideal coordinate of the distorted intersection (P_{gCor_r}) can be calculated by (1).

$$P_{gCor_d} = P_b + (rd_{gCor_r} - rd_{Corb}) * D_{grid_d} \tag{1}$$

It is assumed that grid intersections P_a and P_b whose distance is the largest have no distortion. Its distance is taken as the ideal grid distance (D_{grid_d}).

4. Generated control point pairs $\langle P_{gCor_d}, P_{gCor_r} \rangle$, which are put into set $S(gCor_d, gCor_r) = \{ \langle P_{gCor_d}, P_{gCor_r} \rangle \}$.

This oriented searching method takes advantage of the direction of camber lines in the four different areas, so that all interconnected intersections can be extracted. What's more, those isolated intersections near image edge, like $P_{(7,-6)}$, can also be located by line structure analysis.

2.2 Search optimal center of distortion (CoD)

Some approaches coarsely take the geometric image center as CoD. However, it is indicated that CoD has a considerable offset with respect to the image center [12]. Moreover, the distance of each distorted or undistorted point to CoD can only be calculated by the accurate location of CoD. We adopt a criterion of estimating CoD proposed in [18]: searching in the quarter region of the largest grid, the ideal distances (ideal grid intersections to CoD) are sorted in a monotonic order, if the number of the corresponding distorted distances (distorted grid intersections to CoD) sorted in the corresponding position is maximum, then this candidate point is the optimal CoD.

2.3 Model piecewise polynomial optimization

In our method, lens distortion is modeled based on the relationship of ideal distances and distorted distances. If a single polynomial is used to fit such model, it is fine when lens resolution is low or the distortion is not serious. While, aiming at wide-lens with high resolution and distortion, this single global polynomial method needs higher polynomial

orders with multifold floating-point multiplication, which is quite time-consuming in distortion recovering. Thus, an adaptive piecewise low-order polynomial method is proposed, which reduces polynomial orders and achieve better correction for wide-lens images with large resolution and distortion.

For N pairs in $S_{(gCor_d, gCor_r)}$, calculate distorted distances \bar{r} and ideal distances r , then generate distance set $M(r, \bar{r})$ with r sorted in monotonic order. After that, $M(r, \bar{r})$ is divided into K sub-sets $M_i(r, \bar{r})$, where $r_{n_{i-1}} \leq r \leq r_{n_i}, 1 \leq i \leq K$. And, each sub-set is fitted by least square curve (2).

$$\bar{r} = f_i(r) = \sum_{j=0}^2 a_j^{(i)} r^j, r \in M_i(\bar{r}, r) \tag{2}$$

Where, r_{n_i} is segment position between $f_i(r)$ and $f_{i+1}(r)$. It is assumed that $r_{n_0} = r_0 = 0, r_{n_K} = r_N$. Since CoD has no distortion, the first curve $f_1(r)$ should pass through the origin point, thus $a_0^{(1)} \cong 0$. The last curve $f_K(r)$ fits the distortion in edge regions, so that the maximum point ($r_{\text{symAxis}}, \max(f_K)$) must satisfies the following conditions:

(a) $\max(f_K)$ should be greater than the maximum distorted distance in distorted image (r_{distM}); (b) r_{symAxis} should be no less than the maximum ideal distance in corrected image (r_{examM}). Corrected image size (W', H') and its ideal CoD (CoD_{ideal}) are calculated by similar triangle transform according to distorted distances of four distorted image corners and the last segment curve, shown in Fig. 2.

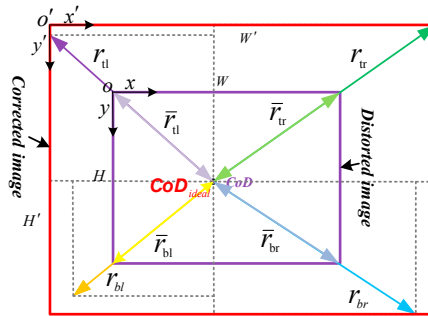


Fig. 2 similar triangle transform for calculating corrected image size

Where, the red minimum enclosing rectangle represents the corrected image size. To avoid zigzag fringes in corresponding areas of segment points and guarantee continuous change of distortion rate, all curves should be smooth at segment points. The fitting quality of curve can be measured by R^2 ranging from 0 to 1. The closer it is to 1, the better the curve fits the observed data. As for $f_i(r)$, R^2 can be calculated by (3).

$$R_i^2 = SSR_i / (SSR_i + SSE_i) \tag{3}$$

Where, $SSR_i = \sum_{j=n_{i-1}}^{n_i} (f_i(r_j) - \bar{r}_{\text{mean}}^{(i)})^2$, $SSE_i = \sum_{j=n_{i-1}}^{n_i} (f_i(r_j) - \bar{r}_j)^2$ and $\bar{r}_{\text{mean}}^{(i)} = (\sum_{j=n_{i-1}}^{n_i} \bar{r}_j) / (n_i - n_{i-1} + 1)$.

Based on analysis above, an inequality constrained optimization problem (4-5) that minimizes two cost functions is established to model the whole distortion.

$$\begin{aligned}
 & \min_{r_n, a_0^{(1)}, 0.8 \leq k \leq 2, 1 \leq i < K} \sum_{i=1}^K \sum_{j=n_{i-1}}^{n_i} [f_i(r_j) - \bar{F}_j]^2, \\
 & \text{s.t. } |f_i(r_{n_i}) - f_{i+1}(r_{n_i})| \leq \lambda, 1 \leq i < K, \\
 & \quad |\arctan(f_i(r_{n_i})) - \arctan(f_{i+1}(r_{n_i}))| \leq \vartheta, 1 \leq i < K, \\
 & \quad |a_0^{(1)}| \leq \delta, R_i^2 > \xi, 1 \leq i < K, \\
 & \quad \max(f_k(r)) > r_{\text{distM}}, f_k^{-1}(\max(f_k(r))) > r_{\text{dreamM}}, \\
 & \quad n_{i+1} \geq n_i + 2, 1 \leq i < K \\
 & \quad \min K, \\
 & \quad \text{s.t. } 1 \leq K \leq \lfloor N/2 \rfloor, \text{ and (4) can be solved.}
 \end{aligned} \tag{4}$$

Minimum pieces, optimal segment points and distortion coefficients can be obtained by solving (4-5) via optimization theories and methods. Through a great deal of experiments, we choose a good parameter option, as follows. Points near CoD may shrink ($a_0^{(1)} > 0$) or expand ($a_0^{(1)} < 0$, but $\delta \in (0, 1)$), this influence can be ignored. To obtain good fitting effects and prevent overfitting, ξ is set to 0.9. Let $\vartheta = 5\pi/180$ (rad) and $\lambda = 2$, a satisfactory smooth at segment points can be guaranteed.

2.4 Obtain Correction Mapping Table(CMT)

To acquire inverse coordinate mapping from corrected image to distorted image and accelerate distortion correction, the CMT with the same size of corrected image is established. Location (x,y) in CMT saves the distorted point coordinate $p'(x,y)$ corresponding to the corrected point $p(x,y)$, which is calculated by similar triangular transformation (6) as shown in Fig. 2.

$$p'(x,y) = CoD + [(p(x,y) - CoD_{\text{ideal}}] \times D_r(p') / D_d(p) \tag{6}$$

Where, the ideal distance of $p(x,y)$ is $D_d(p)$, and $D_r(p')$ is the corresponding distorted distance calculated by (2).

3. Distortion correction

For each corrected point $p(u,v)$ with unknown value, the corresponding distorted point $p'(u,v)$ is obtained directly from CMT. While $p'(u,v)$ may be non-integer, so pixel interpolation is necessary to recover the eventual gray value. Common image interpolation methods are Nearest Neighbor Interpolation, Bilinear Interpolation and Double Cube Interpolation. Considering speed and effect, we choose Bilinear Interpolation method. The recovered gray value of $p'(u,v)$ can be obtained by (7).

$$\begin{aligned}
 I_{p'(u,v)} &= (1-d_u)(1-d_v)I([u],[v]) + d_u(1-d_v)I([u]+1,[v]) \\
 & \quad + d_v(1-d_u)I([u],[v]+1) + d_u d_v I([u]+1,[v]+1)
 \end{aligned} \tag{7}$$

Where, $([u],[v])$, $([u]+1,[v])$, $([u],[v]+1)$, $([u]+1,[v]+1)$ are its four neighbor pixel coordinates, and $d_u = u - [u]$, $d_v = v - [v]$, $[\cdot]$ is a rounding operation. Correction process involves a large number of interpolation calculations with floating-point type, which costs too much time, especially for large image. Therefore, CPU parallel computing or GPU acceleration can be utilized to speed up correction, aiming at real-time applications.

4.. Results and analysis

We implement the proposed method based on VS.Net 2010/C++ development environment. Distorted images are

captured by the camera AEE SD-21 with wide-angle more than 170 degrees and resolution up to 3200x2400. The experimental results for different camera fields are shown in Fig. 3.

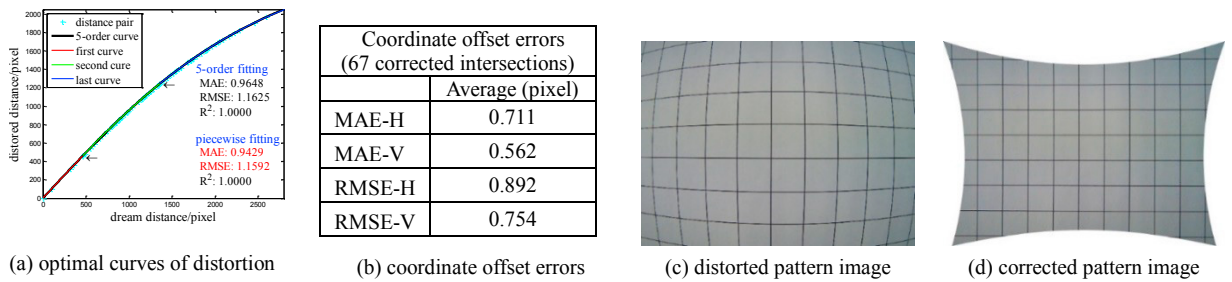


Fig. 3 Small field with high resolution

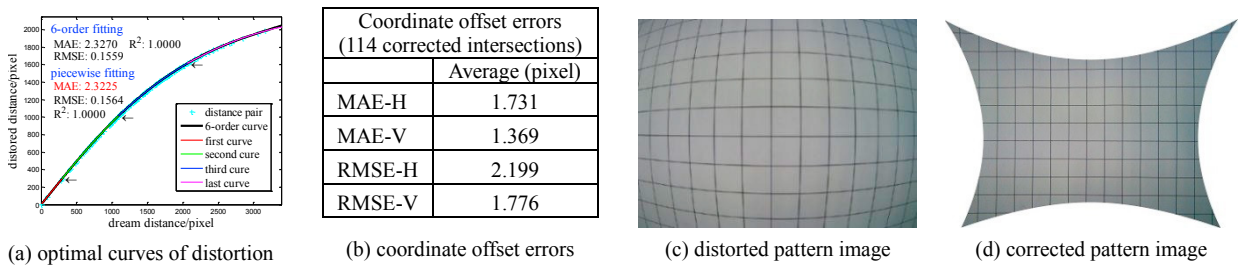


Fig. 4 Medium field with high resolution

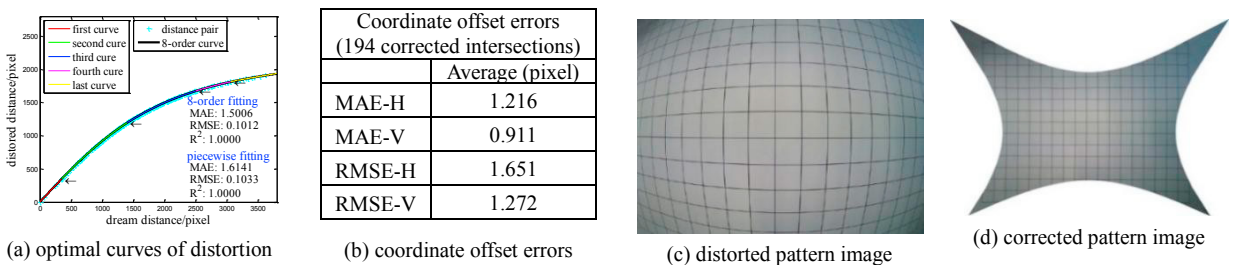


Fig. 5 Large field with high resolution.

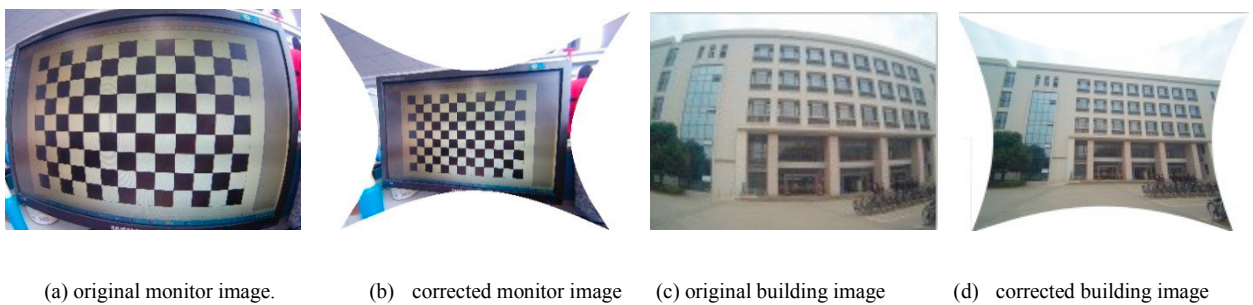


Fig. 6 Scene image with lens distortion corrected by our proposed piecewise method

Note: $MAE = \left\{ \sum_{n=1}^N |f(r_n) - \bar{f}_n| \right\} / N$, $RMSE = \sqrt{\left\{ \sum_{n=1}^N (f(r_n) - \bar{f})^2 \right\} / N}$, $MAE-H(V) = \left\{ \sum_{n=1}^N |P_{H(V)}^{ideal}(n) - P_{H(V)}^{corrected}(n)| \right\} / N$. H and V indicate horizontal

and vertical direction, $RMSE-H(V) = \sqrt{\left\{ \sum_{n=1}^N (P_{H(V)}^{ideal}(n) - P_{H(V)}^{corrected}(n))^2 \right\} / N}$, $P_{H(V)}^{ideal}(n)$ and $P_{H(V)}^{corrected}(n)$ are ideal and corrected intersection

coordinate respectively Under the condition that $\varrho = 5\pi / 180$, $\lambda = 2$, $\xi = 0.9$ and $\delta = 0.25$, from Fig.3(a)-5(a), we can see that all segmented curves have good smooth at segment points, and the minimum segments are adaptive to the extent of distortion. Compared with high-order fitting method, piecewise fitting approach obtains almost equal even better precision according to MAE and RMSE. The proposed method maximizes the use of global image feature, and utilizes the corresponding polynomial curves to fit distortion in different radial annular regions, therefore the entire distorted image can be well corrected and the edge regions with serious distortion are also recovered, seen in Fig. 3(c, d)-5(c, d) and Fig. 6. Since intersections in edge regions of grid pattern are sparse when distorted image is very big, some distortions still exist in these areas. However, it causes little impact on the good total correction quality. Correction errors are shown in Fig. 3(b)-5(b), Average coordinate errors are small with pixel-level in large field no matter in horizontal or vertical direction. But correction errors in medium field are a little bit large, which can be reduced by increasing fitting segments. Error analysis indicates our method owns high correction precision. The above results prove that the proposed method is effective for seriously distorted wide-lens images with high resolution.

5 Conclusion

An adaptive piecewise correction method is proposed to eliminate radial distortion for wide-lens images with high resolution. Automatic extraction of control point pairs is realized only through a single distorted imaged pattern. It reduces the workload of manual operation and improves the accuracy and precision of extraction of control points. The distortion center is estimated by optimal searching criterion, so that we can accurately model the distortion. Than a piecewise polynomial optimization model is built to optimize adaptive segmented distortion coefficients. These optimal segmented coefficients reflect the distortion ranging from the center to the edge of distorted image, which cannot be solved by the single curve fitting function. Finally, an inverse mapping table is set up to speed up correction. The proposed method retains enough information of original image and obtains high-precision correction, besides seriously distorted edge in high-resolution lens images also can be restored.

References

- [1] W. Kim, and C. Kim, "An efficient correction method of wide-angle lens distortion for surveillance systems," ISCAS 2009, IEEE International Symposium on Circuits and Systems, 2009, pp. 3206-3209.
- [2] R. Melo, J. P. Barreto, and G. Falcao, "A new solution for camera calibration and real-time image distortion correction in medical endoscopy-initial technical evaluation," IEEE Transactions on Biomedical Engineering, 2012, vol. 59, no. 8, pp. 634-644.
- [3] X. G. Dong, Y. Zhang, J. L. Liu, et al, "A Fisheye Image Barrel Distortion Correction Method of the Straight Slope Constraint," CISP 2015, the 8th International Congress on Image and Signal Processing, 2015, pp. 173-177.
- [4] J. Weng, P. Cohen, and M. Herniou, "Camera calibration with distortion models and accuracy evaluation," IEEE Transactions on Pattern Analysis and Machine Intelligence, 1992, vol. 14, no. 10, 965-98
- [5] J. Andrade, and L. J. Karam, "Robust radial distortion correction based on alternate optimization," ICIP 2016, IEEE International Conference on Image Processing, 2016, pp. 2956-2960.
- [6] U. Tiwari, U. Mani, S. Paul, et al, "Non-Linear Method Used for Distortion Correction of Fish-eye Lens: Comparative Analysis of Different Mapping Functions," MAMI 2015, International Conference on Man and Machine Interfacing, 2015, pp. 1-5.
- [7] R. Tsai, "A versatile camera calibration technique for high-accuracy 3D machine vision metrology using off-the-shelf TV cameras and lenses," IEEE Journal of Robotics and Automation, 1987, vol. 3, no. 4, pp. 323-344.
- [8] J. Park, S. C. Byun, and B. U. Lee, "Lens Distortion Correction Using Ideal Image Coordinates," IEEE Transactions on Consumer Electronics, 2009, vol. 55, no. 3, pp. 987-991.
- [9] Z. Y. Zhang, "A flexible new technique for camera calibration," IEEE Transactions on Pattern Analysis and Machine Intelligence, 2000, vol. 22, no. 11, pp. 1330-1334.
- [10] A. Fitzgibbon, "Simultaneous linear estimation of multiple view geometry and lens distortion," CVPR 2001, Proceedings of the 2001 IEEE Computer Society Conference on Computer Vision and Pattern Recognition, 2001, pp. 125-132.
- [11] R. A. Wang, T. S. Qiu, and L. T. Shao, "A Simple Method of Radial Distortion Correction with Centre of Distortion Estimation," Journal of Mathematical Imaging and Vision, 2009, vol. 35, no. 3, pp. 165-172.
- [12] R. Hartley, and S. B. Kang, "Parameter-free radial distortion correction with center of distortion estimation," IEEE Transactions on Pattern Analysis and Machine Intelligence, 2007, vol. 29, no. 8, pp. 1309-1321.
- [13] S. H. Lee, S. K. Lee, and J. S. Choi, "Correction of radial distortion using a planar checkerboard pattern and its image," IEEE Transactions on Consumer Electronics, 2009, vol. 55, no. 1, pp. 27-33.

- [14] T. Y. Lee, T. S. Chang, C. H. Wei, et al, “Automatic Distortion Correction of Endoscopic Images Captured With Wide-Angle Zoom Lens,” *IEEE Transactions on Biomedical Engineering*, 2013, vol. 60, no. 9, pp. 2603-2613..
- [15] J. H. Cai, “Automatic Lens Distortion Correction Using Single Images by Finding Reliable Lines for Rectification,” *ICARCV 2014, The 13th International Conference on Control Automation Robotics & Vision*, 2014, pp. 1015-1020
- [16] F. Q. Zhou, Y. C. H. Gao, et al, “Line-based camera calibration with lens distortion correction from a single image,” *Optics and Lasers in Engineering*, 2013, vol. 51, no. 12, pp. 1332-1343.
- [17] T. Y. Lee, T. S. Chang, S. H. Lai, et al, “Wide-angle distortion correction by Hough transform and gradient estimation,” *VCIP 2011, IEEE Conference on Visual Communications and Image Processing*, 2011, pp. 1-4.
- [18] R. Q. Wu, L. L. Wang, and X. R. Cheng, “A Piecewise Correction Method for High-resolution Image of Wide-angle Lens,” *CISP 2013, The 6th International Congress on Image and Signal Processing*, 2013, pp. 331-335.